Transfer RNA fragments replace microRNA regulators of the cholinergic post-stroke immune blockade

Short title: tRF/miR balancers of post-stroke immunity

Katarzyna Winek†[1,2], Sebastian Lobentanzer†[3], Bettina Nadorp[1,4], Serafima Dubnov[1,2], Claudia Dames[5], Gilli Moshitzky[1], Benjamin Hotter[6], Christian Meisel[5], David S Greenberg[2], Sagiv Shifman[7], Jochen Klein[3], Shani Shenhar-Tsarfaty[8], Andreas Meisel[6], Hermona Soreq*[1,2]

†: these authors contributed equally;

[1] The Edmond & Lily Safra Center for Brain Sciences, The Hebrew University of Jerusalem, Jerusalem, Israel

[2] The Alexander Silberman Institute of Life Sciences, The Hebrew University of Jerusalem, Jerusalem, Israel.

[3] Department of Pharmacology, College of Pharmacy, Goethe University, Frankfurt am Main, Germany

[4] The Grass Center for Bioengineering, Benin School of Computer Science and Engineering, The Hebrew University of Jerusalem, Jerusalem, Israel.

[5] The Institute for Medical Immunology, Charité-Universitätsmedizin Berlin, Germany.

[6] NeuroCure Clinical Research, Center for Stroke Research Berlin and The Department of Neurology, Charité-Universitätsmedizin Berlin, Germany

[7] The Department of Genetics, The Hebrew University of Jerusalem, Jerusalem, Israel.

[8] Department of Internal Medicine "C", "D" and "E", Tel Aviv Sourasky Medical Center and Sackler Faculty of Medicine, Tel Aviv University, Tel Aviv, Israel.

* to whom correspondence should be addressed at hermona.soreq@mail.huji.ac.il;

Edmond J. Safra Campus Givat Ram, 91904 Jerusalem, Israel +972 54 882 0629

Abstract

Stroke is a leading cause of death and disability. Recovery depends on balance between inflammatory response and immune suppression, which can be CNS-protective but may worsen prognosis by increasing patients' susceptibility to infections. Peripheral cholinergic blockade of immune reactions fine-tunes this immune response, but its molecular regulators are unknown. Therefore, we sought small RNA balancers of the cholinergic anti-inflammatory pathway in peripheral blood from ischemic stroke patients. Using RNA-sequencing and RT-qPCR, we discovered in patients' blood on day 2 after stroke a "change of guards" reflected in massive decreases in microRNAs (miRs) and increases in transfer RNA fragments (tRFs) targeting cholinergic transcripts. Electrophoresis-based size-selection followed by RT-qPCR validated the top 6 upregulated tRFs in a separate cohort of stroke patients, and independent small RNA-sequencing datasets presented post-stroke enriched tRFs as originating from lymphocytes and monocytes. In these immune compartments, we found CD14+ monocytes to express the highest amounts of cholinergic transcripts. In-depth analysis of CD14+ regulatory circuits revealed minimally overlapping subsets of transcription factors carrying complementary motifs to miRs or tRFs, indicating different roles for the stroke-perturbed members of these small RNA species. Furthermore, LPS-stimulated murine RAW264.7 cells presented dexamethasone-suppressible upregulation of the top 6 tRFs identified in human patients, indicating an evolutionarily conserved and pharmaceutically treatable tRF response to inflammatory cues. Our findings identify tRF/miR subgroups which may co-modulate the homeostatic response to stroke in patients' blood and open novel venues for establishing RNA-targeted concepts for post-stroke diagnosis and therapeutics.

Keywords

acetylcholine; ischemic stroke; microRNA; immunology; transfer RNA fragment

Introduction

The increasing incidence of ischemic stroke is a global burden of growing dimensions, accounting for 12 of the 15 million strokes annually, and leaving most of the surviving patients permanently disabled(1). The immune system is one of the main players in the pathophysiology of stroke. Brain injury dampens immune functions in the periphery, which limits the inflammatory response and infiltration of immune cells into the CNS and may pose a neuroprotective mechanism in stroke patients. Importantly, this systemic immunosuppression simultaneously increases the risk of infectious complications(2), e.g. by inducing lymphocyte apoptosis and decreasing production of pro-inflammatory cytokines (lymphocytic IFNγ and monocytic TNFα)(3). Therefore, post-stroke recovery largely depends on a delicate balance between inflammation, which exacerbates the severity of symptoms, and the post-stroke suppression of immune functions, which increases the susceptibility to infections(3). This involves incompletely understood molecular regulators of cholinergic and sympathetic signaling and the hypothalamus-pituitary-adrenal gland axis (HPA). Among other processes, brain injury leads to activation of the vagus nerve, which mediates anti-inflammatory signaling through the cholinergic efferent fibers and the noradrenergic splenic nerve. Binding of acetylcholine (ACh) to the nicotinic alpha 7 receptors on monocytes/macrophages decreases the production of proinflammatory cytokines(4) in a manner susceptible to suppression by microRNA (miR) regulators of cholinergic signaling, such as miR-132(5). We hypothesized that this and other small RNA fine-tuners of innate immune responses, including miRs and the recently re-discovered transfer RNA (tRNA) fragments (tRFs) may contribute to regulation of post-stroke processes.

Both miRs and tRFs may control entire biological pathways, such that their balanced orchestration could modulate brain-induced systemic immune functioning. miRs are small non-coding RNAs whose expression requires transcription yet can be rapidly induced, enabling

degradation and/or translational suppression of target genes carrying a complementary motif. One miR may suppress the expression of many targets involved in the same biological pathway, and many miRs may co-target the same transcripts, enabling cooperative suppression. Hence, miR regulators of ACh signaling may shape the role of ACh in both cognitive function and systemic inflammation(5, 6).

Recent reports highlight tRNA as another major source of small noncoding RNA(7), including tRNA halves (tiRNAs) and smaller tRNA fragments - tRFs. tiRNAs are created by angiogenin cleavage at the anticodon loop(8) raising the possibility that the post-stroke angiogenin increase might change their levels(9). Among other functions(10, 11), smaller fragments derived from the 3'- or 5'-end of tRNA (3'-tRF/5'-tRF) or internal tRNA parts (i-tRF) may incorporate into Argonaute (Ago) protein complexes and act like miRs to suppress their targets(12). Differential expression of tRFs was reported under hypoxia, oxidative stress, ischemic reperfusion(8, 13) and in epilepsy(14), which are all involved in ischemic stroke complications. tRFs may be generated via enzymatic degradation of tRNA, independent of de-novo transcription, which implies that tRF levels may be modulated more rapidly than miR levels. However, whether brain-body communication and immune suppression after ischemic stroke in human patients involves blood tRF changes has not yet been studied.

Taking into consideration that the cholinergic system is one of the controllers of immune functions, we looked for changes in the levels of miR and tRF regulators, with a specific focus on those which may control the ACh-mediated suppression of post-stroke immune functions. We performed small and long RNA-sequencing of whole blood samples collected from stroke patients two days after stroke onset, mined RNA-sequencing datasets of blood cell transcripts and sought potential links between perturbed miRs and tRFs, post-stroke immune responses and the cholinergic anti-inflammatory pathway.

Results

A cholinergic-targeting shift from miRs to tRFs in post-stroke patients' blood

To seek post-stroke small RNA regulators of body-brain communication, we first performed small RNA-sequencing of whole blood samples collected on day 2 after ischemic stroke from 33 male patients of the PREDICT cohort (484 participants)(15) and 10 age- and sex-matched controls (Figure 1A; see demographic data in Data file S1). Principal Component Analysis (PCA) of the differentially expressed (DE) small RNAs completely segregated the stroke and control groups (Fig. 1B). The respective direction of change among the two small RNA classes involved a statistically significant decline in miRs and a parallel increase in tRFs, indicating a 'change of guards' from miRs to tRFs. Specifically, 87% of the 143 DE tRFs were upregulated, whereas 63% of the 420 DE miRs were downregulated (Benjamini-Hochberg corrected $p < 0.05$; Fig. 1C, D). Of the 143 DE tRFs, 87 were 3'-tRFs, and 30 of those (all upregulated) were derived from alanine binding tRNA (Supplementary Fig. S1), indicating non-arbitrary fragment generation.

Notably, the 420 DE miRs included several miRs known to be perturbed in stroke: miR-532-5p (logFC = -2.27, p = 1.81e-33) (16), miR 148a-3p (logFC = -2.30, p = 9.61e-19) and let-7i-3p (logFC = -1.07, p = 4.31e-04) (17). To test the potential involvement of miRs and tRFs in regulating the cholinergic anti-inflammatory pathway after stroke, we performed targeting analysis of DE miRs and tRFs towards cholinergic transcripts (Supplementary Methods, for a complete list of cholinergic genes see Data File S2) via an in-house integrative database (*miRNeo*)(18) containing comprehensive transcription factor(TF)- and miR-targeting data, complemented by de-novo prediction of tRF-targeting using TargetScan(19). A restrictive approach identified subsets of 131/420 miRs and 64/143 tRFs containing complementary motifs to at least five cholinergic-associated transcripts each (further termed "Cholino-miRs" and "Cholino-tRFs", Fig. 1C, D, Supplementary Fig. S2, full lists in Data files S3 and S4). Permutation targeting analysis showed an enrichment of cholinergic targets for both DE miRs (100 000 permutations, p = 0.0036) and DE tRFs (100 000 permutations, p = 2e-05). Further indicating non-random generation of these

fragments, the tRFs identified in our dataset clustered into oligonucleotide families with high sequence homology via t-distributed stochastic neighbor embedding (t-SNE) (Fig. 1E), including families known to associate with Ago and suppress growth and proliferation via post-transcriptional downregulation in lymphocytes (e.g. tRF-22-WE8SPOX52 from tRNAGly)(20) and metastatic cancer cells (tRF-18-HR0VX6D2 from tRNALeu)(21). This supported our prediction that the concomitant elevation of tRF- and decline of miR-levels in post-stroke blood could contribute to the post-stroke changes in cholinergic signaling pathways.

To further challenge our findings, we validated the expression levels of prominently DE tRFs identified by RNA sequencing in a separate cohort of PREDICT patients(15). Standard qPCR techniques cannot distinguish between the full length tRNA molecules and their 3'-tRF cleavage products. Therefore, to experimentally validate tRF changes (Fig. 2A) we implemented an electrophoresis size selection-based strategy followed by cDNA synthesis from the selected small RNAs and RT-qPCR (maximum 25 nt, Fig. 2B). This procedure validated the top six upregulated tRFs identified in RNA-sequencing data (tRF-22-WEKSPM852, tRF-18-8R6546D2, tRF-18-HR0VX6D2, tRF-18-8R6Q46D2, tRF-22-8EKSP1852 and tRF-22-WE8SPOX52; according to count-change, see Supplementary Methods, Fig. 2A and C) and demonstrated significant increases accompanied by higher variability in the blood levels of these tRFs in post-stroke patients compared to controls.

Stroke-regulated whole blood tRFs reflect distinct immune cell compartments

To clarify the distribution of stroke-perturbed tRFs among the immunologically relevant blood cell types, we mined an RNA-sequencing dataset comprising sorted cell populations collected from healthy volunteers: CD4+ T helper cells, CD8+ T cytotoxic cells, CD56+ NK cells, CD19+ B cells, CD14+ monocytes, CD15+ neutrophils, CD235a+ erythrocytes, serum, exosomes, and whole blood (450 samples in total, (22)) (Fig. 3A). Predicting that log-normal distribution of the counts in different samples would point towards biological significance, we categorized all tRFs found in this dataset into present/absent in a specific blood compartment (without introducing a limit for

counts, see Methods, Fig. 3B). Two main clusters of specific blood compartments could be identified based on their specific tRF profile: a) monocytes, B-, T- and NK cells; b) neutrophils, whole blood, serum, exosomes and erythrocytes (Supplementary Fig. S3). Further, we distinguished eight tRF sub-clusters, based on the presence/absence of specific tRFs in blood compartments (Fig. 3C), with cluster four comprising molecules expressed specifically in monocytes, B-, T-, and NK-cells, and cluster seven consisting of tRFs expressed only in monocytes.

Using the presence/absence measure for analyzing the post-stroke DE tRFs (Fig. 3D, Supplementary Fig. S4 for the top 20 stroke DE tRFs), we detected 77 DE tRFs from the PREDICT dataset as expressed in immune cells (Fig. 3E, a detailed list of tRFs and affiliated clusters in Data File S5), including 10 Cholino-tRFs. Notably, tRFs previously shown to function post-transcriptionally in a miR-like manner (e.g. tRF-22-WE8SPOX52 from tRNAGly(20) and tRF-18-HR0VX6D2 from tRNALeu, alias miR-1280(21)) segregated into whole blood, monocyte, T-, B-, and NK-cell compartments rather than into erythrocyte, serum or exosome compartments. Thus, the post-stroke modified tRFs may be functionally involved in regulating the leukocytic post-stroke response.

CD14+ monocytes show highest transcriptional activation towards cholinergic genes

The enrichment of DE Cholino-miRs and Cholino-tRFs identified in the PREDICT dataset and the contribution of the cholinergic anti-inflammatory pathway to peripheral immunosuppression called for pinpointing the immune compartment(s) in which these small RNAs might affect post-stroke immune suppression. Analysis of long RNA regulatory circuits specific to blood-borne leukocytes (Fig. 4A)(23) identified CD14+ monocytes as the main cell type expressing cholinergic core and receptor genes (Data File S2, Fig. 4B). To challenge the relevance of this effect for leukocyte features, we performed long RNA-sequencing in blood samples from 20 stroke patients from the PREDICT study and 4 controls. This showed 204 upregulated and 490 downregulated long RNA transcripts. Gene ontology (GO) enrichment analyses of the most implicated genes yielded highly

specific terms relevant to innate immunity, vascular processes, and cholinergic links (Fig. 4C, list of all significant terms in Supplementary Table 1). More specifically, terms linked to innate immune processes in post-stroke blood involved *responses to LPS mediated by interferons and other cytokines* (Figure 4C, left-hand side); vascular processes comprised *platelet activation and degranulation*, *control of cell-cell adhesion*, and *regulation of angiogenesis* (Figure 4C, right-hand side). Intriguingly, differentially regulated genes also showed involvement in *response to organophosphorus,* which are known acetylcholinesterase (AChE) inhibitors, implying a cholinergic participation.

tRFs may suppress inflammation and cholinergic-associated transcription factors alone or in cooperation with miRs

Cellular responses to different stimuli are coordinated by cell type-specific transcriptional regulatory circuits. To facilitate understanding of the role of miRs and tRFs in regulating the transcriptional state of CD14+ monocytes after stroke, we generated a monocyte-specific transcriptional interaction network of small RNAs targeting transcription factors (via *miRNeo*)(18), combined with differential expression of long and small RNAs from the PREDICT cohort (Fig. 5A). Notably, the force-directed network of all TFs active in CD14+ monocytes self-segregated to form two distinct clusters of TFs which were primarily targeted either by miRs or tRFs, including numerous TFs DE in stroke patient blood (Fig. 5B). The gradually divergent targeting of these TFs by miRs and/or tRFs implied largely separate domains of regulation by either small RNA species (Fig. 5C). Among the implied TFs are proteins known for their influence on cholinergic genes as well as their involvement in inflammation, such as STAT1 or KLF4(24, 25). Intriguingly, 8 DE TFs were not predicted to be targeted by any miR or tRF present in CD14+ monocytes (Fig. 5D).

Next, we aimed to test if the stroke-induced tRFs are involved in the inflammatory response of monocytes and macrophages. For this purpose, we subjected murine RAW264.7 cells to LPS-stimulation with or without dexamethasone suppression of their inflammatory reactions (Fig. 5E).

By 18h after LPS stimulation, RT-qPCR analysis based on size-selection (for <50 nt fragments) detected pronounced upregulation of the top 6 post-stroke upregulated tRFs (Fig. 5F). Moreover, dexamethasone suppression of the LPS response prevented increase of those tRFs, along with a diminished inflammatory response (Supplementary Fig. S5). Predicted targets of these molecules comprise members of mitogen-activated protein kinases (MAPK) and tumor necrosis factor receptor-associated factors (TRAF) (see Data File S6), further pointing towards their regulatory role in response to inflammatory stimuli. Together, these findings demonstrate evolutionarily conserved increases of stroke-induced tRFs under pro-inflammatory insults and dexamethasone-mediated suppression of their generation in mononuclear immune cells.

Discussion

We discovered a stroke-induced decline of miRs and concomitant elevation of tRFs in whole blood, and demonstrated that this shift may modulate the post-stroke cholinergic blockade of immune function. To validate our RNA-seq findings of tRNA fragments in a way that circumvents the ambiguous detection of full-length tRNA, we developed and used a size selection-based RT-qPCR test in an independent cohort of patients. Mining transcriptomic datasets identified CD14+ monocytes as highly involved in the cholinergic control of immunity, demonstrated that the stroke-induced tRFs may target specific monocytic TFs, and showed that at least some of those tRFs may actively control processes linked to inflammatory responses. Moreover, several of the stroke-induced tRFs were also induced in LPS-exposed murine macrophages in a dexamethasone-suppressible manner, supporting the notion that the elevation of tRFs is an evolutionarily conserved mechanism. This novel concept for the fine-tuning of post-stroke immune response opens new venues for post-stroke diagnostics and therapeutics.

The cholinergic anti-inflammatory reflex plays a substantial role in regulating peripheral immune responses after CNS injury, along with the HPA axis and sympathetic signaling(3). Excessive cholinergic responses suppress pulmonary innate immunity, including macrophage and alveolar epithelial cell responses and facilitate the development of pneumonia(26), a major factor of non-recovery(27). However, while reduced AChE activities in post-stroke patients' serum associate with poor survival(28), stroke-induced immunosuppression may be brain-protective(2), calling for caution when considering therapeutic boosting of immune reaction in the periphery to limit infections. Therefore, an in-depth understanding and characterization of the molecular regulators of immune responses and the cholinergic pathway after CNS-injury is of utmost importance.

Translational control is important for regulating stress and immunity(29), and tRFs may be rapidly produced by regulated nuclease cleavage of pre-existing tRNAs in a "burst-like" fashion, which makes them particularly appropriate for handling acute situations. Recent reports demonstrate production of 3'-tRFs by specific nucleases, and 3'- and 5'-tRNALeu fragments were shown to regulate T cell activation(30). Furthermore, tRFs can perform different molecular roles, including Ago-mediated suppression of target genes carrying complementary sequence motifs(12). At least two of the stroke-induced tRFs upregulated after LPS stimulation show miR-like function: tRF-22-WE8SPOX52 regulates B cell growth via suppressing the expression of Replication Protein A1 (RPA1)(20) and a 17 nucleotides-long fragment of tRF-18-HR0VX6D2 limits cancer cell proliferation by impacting the cholinergic-regulating Notch signaling pathway(21). Interestingly, miR-1260b, identified in our study and by others as perturbed post-stroke(31) differs from tRF-18-HR0VX6D2 by one nucleotide at position 9 and an additional nucleotide at the 3'-end (Supplementary Fig. S6), which indicates that miR-1260b may actually be a tRF(32), and calls for further investigations.

Apart from their miR-like activities, tRFs may have other functions. For instance, tRNALeu-CAG fragments facilitate translation and ribosome biogenesis(11), whereas tRNAGly, tRNAGlu, tRNAAsp and tRNATyr-derived tRFs displace RNA-binding proteins leading to mRNA

destabilization(10). Therefore, potential functions of stroke-perturbed tRFs other than Ago-mediated suppression of gene expression should be further tested.

Like tRFs, miRs may exert diverse effects depending on their mRNA target site, yet their primary mode of action is translational repression. We found 420 DE miRs, some of which are known to be influenced by CNS injury, in the blood of post-stroke PREDICT patients. A recent whole blood microarray survey identified 15 miRs, including 11 replicated in our study, to be suppressed within less than 72 hours in intracerebral hemorrhage patients compared to controls(33). All of those miRs target multiple immune-related pathways, including Toll-like receptors, neurokine/JAK-STAT signaling and natural killer cell-mediated cytotoxicity(33). We conclude that the observed changes in both miRs and tRFs may be functionally relevant for post-stroke immunity and recovery prospects.

We have found CD14+ monocytes to be the most prominent immune subpopulation in cholinergic responses. The role of monocytes in stroke-associated infections has been already established: post-stroke responses include prolonged monocytosis, deactivation and functional impairment of circulating monocytes/macrophages observed in experimental models(34) and human patients(35). Moreover, stroke leads to over-production of CD14++ CD16- (classical) and CD14++ CD16+ (intermediate) monocytes with simultaneous decrease in CD14+CD16++ (nonclassical) monocytes, which correlates with stroke-associated infection(36). The response to stroke in blood cells follows specific kinetics: day 2 post ischemia features an increase in STAT3 phosphorylation in monocyte subsets when compared to long-term immune responses, which is a hallmark of innate immune reaction to tissue injury that is also detected in patients after major surgery(37). Conversely, STAT3 signaling is linked to immunosuppression in monocytic myeloid-derived suppressor cells (M-MDSC, CD11b+HLA-DR-CD14+CD15-)(38), but causes immune stimulation in monocytes(37). Therefore, the biological activities of stroke-induced tRFs may also be context-specific.

Stroke is characterized by an initial inflammatory response followed by immunosuppression facilitated by, among others, the cholinergic anti-inflammatory reflex(3). Therefore, the tRFs and Cholino-tRFs in particular may offer new mechanisms of homeostatic fine-tuning in response to cerebral ischemia. Further, not only the peripheral but also the central immune response at the site of the injury is of great importance for stroke prognosis. Brain injury triggers activation of microglia and infiltration of peripheral immune cells, including monocyte-derived macrophages, which accumulate at the lesion site 3-7 days after stroke(36). Experimental evidence highlights essential roles of these cells in CNS-repair processes and neuronal protection(39, 40), and our own studies indicate small RNA-regulated cross-talk between neuronal and immunological regulation by JAK/STAT-related mechanisms(18). Our current study presents tRFs as potential players in regulation of these neuroinflammatory responses.

Our targeting predictions indicate that the stroke-induced tRFs and suppressed miRs may both regulate monocytic transcriptional states and imply the existence of exclusive and shared regulatory domains between these two small RNA species. Thus, the post-stroke “change of guards” in the small RNA response may lead to preferential de-repression of miR targets and concomitant repression of tRF targets. The de-repression of miR targets may hence be as pivotal for regulating the initial inflammatory response and subsequent peripheral immunosuppression as the tRF elevation we identified. For example, KLF4, identified as down-regulated in our sequencing dataset, is involved in controlling the macrophage response to LPS(25) and the differentiation of monocytes towards an inflammatory phenotype(41). Therefore, a decrease in miRs targeting this TF may contribute to pro-inflammatory monocytic response observed in the initial phase of stroke. Similarly, MAFB is essential in facilitating the clearance of damage-associated molecular patterns (DAMPs) in the ischemic brain, and, consequentially, limiting the inflammatory response while supporting recovery(42). MAFB de-repression in peripheral immune cells may be a mechanism supporting monocyte infiltration of the brain. Conversely, STAT1 and

ATF3 may be preferentially repressed due to their targeting by tRFs. STAT1 is essential in IFN- and IL-6-mediated inflammatory response, and ATF3 is similarly induced by IFNs and contributes to STAT activity via inhibition of STAT-dephosphorylating phosphatases(43, 44). Additionally, ATF3 down-regulates AChE expression during stress(45). Whether these processes contribute to body homeostasis after the traumatic event, or rather to pathologic derailment of immune function, requires detailed kinetic studies of circulating monocytes and brain-infiltrating monocyte-derived macrophages, with simultaneous profiling of short and long transcripts.

While the specific roles of tRFs in regulating local neuroinflammatory responses and functional modulation of specific peripheral monocyte subsets remain to be elucidated, our findings point towards tRFs/miRs as interchangeable regulators of post-stroke immune responses and potential biomarkers for increased infection risk in these patients. The cumulative role of tRFs and miRs as general post-traumatic mediators of CNS-immune communication thus calls for seeking small RNAs, and tRFs in particular, as involved in other traumatic pathologies such as spinal cord injury, traumatic brain injury, concussion, as well as neuroinflammatory brain diseases.

Materials and Methods

Expanded methods can be found in the online supplement.

Clinical cohort

PREDICT was a prospective multi-center study with sites in Germany and Spain (www.clinicaltrials.gov, NCT01079728)(15) that analyzed 484 acute ischemic stroke patients. Patients underwent daily screenings for stroke-associated pneumonia, dysphagia and inflammation markers and their clinical outcome was recorded 3 months post-stroke. To exclude very severe cases of stroke, we only considered for sequencing samples from patients with

modified Rankin Scale (mRS) values of 3 and below at discharge from the hospital, leaving n=240 relevant cases. Blood was collected into RNA stabilizing tubes (Tempus Blood RNA tubes, Applied Biosystems™) on each day of hospitalization. Blood samples collected on the 2nd day were subjected to small and long RNA-sequencing, with time from stroke occurrence to blood withdrawal varying between 0.94 to 2.63 days (average: 1.98 days). Blood samples from age- and ethnicity-matched healthy controls were obtained at matched circadian time from donors with ethical approvals from institutional review boards (ZenBio, North Carolina, USA).

RNA extraction, quality control and sequencing

RNA was extracted from 3 ml of whole blood of 484 PREDICT patients using Tempus Spin RNA isolation kit (Invitrogen, Thermo Fisher Scientific, Waltham MA, USA). Pre-sequencing Bioanalyzer 6000 (Agilent, Santa Clara CA, USA) tests showed high RNA quality (RIN values 7.9-9.9, median 8.8). Libraries constructed from 600 ng total RNA of 43 samples were subjected to small RNA-sequencing (NEBNext® Multiplex Small RNA library prep set for Illumina, New England Biolabs, Ipswich MA, USA), and 24 of the small RNA-sequenced samples served for PolyA-selected long mRNA sequencing (1000 ng total RNA per sample, TruSeq RNA library preparation kit (Illumina, San Diego CA, USA)). Sequencing (24 or 12 samples per flow cell for small and long RNAs, respectively) was performed on the Illumina NextSeq 500 platform at the Hebrew University's Center for Genomic Technologies.

Alignment and count table generation of RNA sequencing reads

Quality control was performed using FastQC, version 0.11.2. Flexbar(46) (with parameters "-q TAIL -qf Sanger -qw 4 -min-read-length 16")(47) served for adapter trimming and quality based filtering of all raw reads. Long RNA was aligned to the human reference transcriptome (ENSEMBL GRCh38 release 79) using salmon(48) with default parameters. Small RNA was aligned to the miRBase version 21 using miRExpress 2.1.4(49) with default parameters but skipping adapter trimming for miR expression, and to the tRNA transcriptome using the MINTmap

pipeline(50) with default parameters for tRF expression (using only reads mapping exclusively to the tRNA space). Raw gene-expression data of small and long RNA sequencing and technical covariates are available via the GEO database (GEO accession number GSE112803).

Size selection for tRF quantification

Standard RT-qPCR methods do not allow to distinguish between full length tRNA molecules and 3'tRFs. To exclude longer RNA species in the RT-qPCR quantifications, we performed RNA size selection on 15% TBE-Urea-Polyacrylamide gels, selecting only RNA molecules ≤ 25 nucleotides for validations in the clinical cohort and ≤ 50 nucleotides for the assessment of tRF expression in LPS-stimulated RAW 264.7 cells. Detailed description can be found in the Supplementary Methods.

Analysis of the presence/absence of specific tRFs in blood compartments

In descriptive analysis of small RNA expression, a threshold (e.g., at least 5 counts in at least 80% of samples) is often used to define presence or absence of small RNAs. However, since this definition relies heavily on sequencing depth, and depth can vary widely even in methodically robust sequencing experiments depending on a large number of variables, we defined our own test for descriptive analysis of presence or absence of lowly expressed small RNAs in each of the sample types. Briefly, this definition comprises estimation of a log-normal distribution on the expression profile of the small RNA across all samples in the individual cell types, and a statistical test to refute the null hypothesis that the distribution is in fact log-normal. For each small RNA, the distribution mean and standard deviation of the expression values per cell type were estimated using the *fitdist* function of the R/fitdistrplus package(51). The count distribution was then tested against a log-normal distribution with the estimated mean and standard deviation via the R implementation of the Kolmogorov-Smirnov test, with a cutoff of 0.1. The small RNA was defined as present if the test failed to reject the null hypothesis (see Supplementary Fig. S4 for examples).

Cell culture experiments

Murine RAW264.7 cells (ATCC TIB-71) cultured according to standard protocols in Dulbecco's Modified Eagle's Medium supplemented with 10% Fetal Calf Serum, 1% Penicillin-Streptomycin-Amphotericin B and 1% L-Glutamine were collected using cell scraper and stimulated with lipopolysaccharide (LPS from *E.coli*, Sigma Aldrich, St. Louis, USA) following modified protocol by Bartosh et al.(52) . Briefly, $2x10^5$ cells were stimulated with 100 ng/ml LPS +/- 0.5 μM dexamethasone per well (Sigma Aldrich, St. Louis, USA) in 12-well cell culture plates. Cells were collected in Tri-Reagent (Sigma Aldrich, St. Louis, USA) 18h after LPS stimulation and RNA was isolated using miRNeasy kit (Qiagen, Hilden, Germany). For the size selection 1 μg of total RNA was used and cDNA was synthesized from 500 pg size selected RNA using qScript microRNA cDNA Synthesis Kit (Quanta Biosciences, Beverly MA, USA) and following standard protocol (for further details see Supplementary Methods). Data presented in the manuscript is derived from 3 independent experiments (2 of them with dexamethasone treatment) with 2-4 technical replicates in each group.

Statistical analysis

Data analysis was performed using R (version 3.4.1). FDR correction was applied whenever applicable, and qPCR data was analyzed using Bio-Rad CFX Maestro software (Bio-Rad, Version 4.1.2433.1219) and GraphPad Prism 8.0 (GraphPad Prism Software Inc., San Diego, USA).

Acknowledgments

The authors would like to thank Dr. Simonas Juzenas (Saarbrücken) and Prof. Andreas Keller (Saarbrücken/Stanford) for their support concerning the blood compartments RNA-sequencing dataset and Dr. Iftach Shaked (San Diego) for fruitful discussions.

Funding

This study was supported by the European Research Council Advanced Award 321501, the Israel Science Foundation grant 1016/18, the Israeli Ministry of Science, Technology and Space Grant No. 53140 (to H.S), as well as by the German Research Foundation (Exc257, TR84, SFB/TRR167) (to A.M and C.M) and the Einstein Foundation, Berlin (to A.M and H.S). Further support was provided by a NeuroCure visiting fellowship (to H.S), as well as by Edmond and Lily Safra Center of Brain Science (ELSC) post-doctoral fellowships to S.S-T and K.W. K.W is a Shimon Peres Post-doctoral Fellow at the ELSC and S.L received an ELSC fellowship for visiting PhD students.

References

1. E. J. Benjamin, *et al.*, Heart Disease and Stroke Statistics-2018 Update: A Report From the American Heart Association. *Circulation* **137**, e67–e492 (2018).
2. U. Dirnagl, *et al.*, Stroke-induced immunodepression: experimental evidence and clinical relevance. *Stroke* **38**, 770–773 (2007).
3. C. Meisel, J. M. Schwab, K. Prass, A. Meisel, U. Dirnagl, Central nervous system injury-induced immune deficiency syndrome. *Nat Rev Neurosci* **6**, 775–786 (2005).
4. L. V. Borovikova, *et al.*, Vagus nerve stimulation attenuates the systemic inflammatory response to endotoxin. *Nature* **405**, 458–462 (2000).
5. I. Shaked, *et al.*, MicroRNA-132 potentiates cholinergic anti-inflammatory signaling by targeting acetylcholinesterase. *Immunity* **31**, 965–973 (2009).
6. H. Soreq, Checks and balances on cholinergic signaling in brain and body function. *Trends Neurosci* **38**, 448–458 (2015).
7. A. G. Torres, O. Reina, C. Stephan-Otto Attolini, L. Ribas de Pouplana, Differential expression of human tRNA genes drives the abundance of tRNA-derived fragments. *Proc. Natl. Acad. Sci. U. S. A.* **116**, 8451–8456 (2019).
8. S. Yamasaki, P. Ivanov, G. F. Hu, P. Anderson, Angiogenin cleaves tRNA and promotes stress-induced translational repression. *J Cell Biol* **185**, 35–42 (2009).
9. L. Huang, H. Guo, M. Cheng, Y. Zhao, X. Jin, The kinetic change of the serum angiogenin level in patients with acute cerebral infarction. *Eur. Neurol.* **58**, 224–227 (2007).
10. H. Goodarzi, *et al.*, Endogenous tRNA-Derived Fragments Suppress Breast Cancer Progression via YBX1 Displacement. *Cell* **161**, 790–802 (2015).
11. H. K. Kim, *et al.*, A transfer-RNA-derived small RNA regulates ribosome biogenesis. *Nature* **552**, 57 (2017).
12. P. Kumar, J. Anaya, S. B. Mudunuri, A. Dutta, Meta-analysis of tRNA derived RNA

fragments reveals that they are evolutionarily conserved and associate with AGO proteins to recognize specific RNA targets. *BMC Biol* **12**, 78 (2014).

13. Q. Li, *et al.*, TRNA-Derived Small Non-Coding RNAs in Response to Ischemia Inhibit Angiogenesis. *Sci. Rep.* **6**, 20850 (2016).
14. M. C. Hogg, *et al.*, Elevation of plasma tRNA fragments precedes seizures in human epilepsy. *J. Clin. Invest.* **129**, 2946–2951 (2019).
15. S. Hoffmann, *et al.*, Stroke-induced immunodepression and dysphagia independently predict stroke-associated pneumonia - The PREDICT study. *J Cereb Blood Flow Metab* **37**, 3671–3682 (2017).
16. P. Li, *et al.*, Identification of circulating microRNAs as potential biomarkers for detecting acute ischemic stroke. *Cell Mol Neurobiol* **35**, 433–447 (2015).
17. G. C. Jickling, *et al.*, microRNA Expression in Peripheral Blood Cells following Acute Ischemic Stroke and Their Predicted Gene Targets. *PLoS One* **9** (2014).
18. S. Lobentanzer, G. Hanin, J. Klein, H. Soreq, Integrative Transcriptomics Reveals Sexually Dimorphic Control of the Cholinergic/Neurokine Interface in Schizophrenia and Bipolar Disorder. *Cell Rep.* **29**, 764-777.e5 (2019).
19. V. Agarwal, G. W. Bell, J. W. Nam, D. P. Bartel, Predicting effective microRNA target sites in mammalian mRNAs. *Elife* **4** (2015).
20. R. L. Maute, *et al.*, tRNA-derived microRNA modulates proliferation and the DNA damage response and is down-regulated in B cell lymphoma. *Proc. Natl. Acad. Sci. U. S. A.* **110**, 1404–9 (2013).
21. B. Huang, *et al.*, Molecular and Cellular Pathobiology tRF/miR-1280 Suppresses Stem Cell-like Cells and Metastasis in Colorectal Cancer (2017) https:/doi.org/10.1158/0008-5472.CAN-16-3146 (January 30, 2019).
22. S. Juzenas, *et al.*, A comprehensive, cell specific microRNA catalogue of human peripheral blood. *Nucleic Acids Res.* **45**, 9290–9301 (2017).
23. D. Marbach, *et al.*, Tissue-specific regulatory circuits reveal variable modular perturbations across complex diseases. *Nat. Methods* **13**, 366–370 (2016).
24. K. Shuai, *et al.*, Interferon activation of the transcription factor Stat91 involves dimerization through SH2-phosphotyrosyl peptide interactions. *Cell* **76**, 821–828 (1994).
25. M. W. Feinberg, *et al.*, Kruppel-like factor 4 is a mediator of proinflammatory signaling in macrophages. *J. Biol. Chem.* **280**, 38247–38258 (2005).
26. O. Engel, *et al.*, Cholinergic Pathway Suppresses Pulmonary Innate Immunity Facilitating Pneumonia after Stroke. *Stroke* **46**, 3232–3240 (2015).
27. O. Finlayson, *et al.*, Risk factors, inpatient care, and outcomes of pneumonia after ischemic stroke. *Neurology* **77**, 1338–1345 (2011).
28. E. Ben Assayag, *et al.*, Serum cholinesterase activities distinguish between stroke patients and controls and predict 12-month mortality. *Mol Med* **16**, 278–286 (2010).
29. C. A. Piccirillo, E. Bjur, I. Topisirovic, N. Sonenberg, O. Larsson, Translational control of immune responses: from transcripts to translatomes. *Nat. Immunol.* **15**, 503–511 (2014).
30. N.-T. Chiou, R. Kageyama, K. M. Ansel, Selective Export into Extracellular Vesicles and Function of tRNA Fragments during T Cell Activation. *Cell Rep.* **25**, 3356-3370.e4 (2018).
31. J. R. Tan, *et al.*, Blood microRNAs in low or no risk ischemic stroke patients. *Int. J. Mol. Sci.* **14**, 2072–84 (2013).
32. N. C. T. Schopman, S. Heynen, J. Haasnoot, B. Berkhout, A miRNA-tRNA mix-up: tRNA origin of proposed miRNA. *RNA Biol.* **7**, 573–576 (2010).
33. X. Cheng, *et al.*, MicroRNA and their target mRNAs change expression in whole blood of patients after intracerebral hemorrhage. *J. Cereb. Blood Flow Metab.*, 0271678X1983950 (2019).
34. L. McCulloch, A. Alfieri, B. W. McColl, Experimental stroke differentially affects discrete subpopulations of splenic macrophages. *Front. Immunol.* **9**, 1108 (2018).
35. X. Urra, *et al.*, Monocyte subtypes predict clinical course and prognosis in human stroke. *J. Cereb. Blood Flow Metab.* **29**, 994–1002 (2009).
36. A. ElAli, N. J. LeBlanc, The role of monocytes in ischemic stroke pathobiology: New

avenues to explore. *Front. Aging Neurosci.* **8** (2016).
37. A. S. Tsai, *et al.*, A year-long immune profile of the systemic response in acute stroke survivors. *Brain* **142**, 978–991 (2019).
38. L. Cassetta, *et al.*, Deciphering myeloid-derived suppressor cells: isolation and markers in humans, mice and non-human primates. *Cancer Immunol. Immunother.* **68**, 687–697 (2019).
39. S. Wattananit, *et al.*, Monocyte-derived macrophages contribute to spontaneous long-term functional recovery after stroke in mice. *J. Neurosci.* **36**, 4182–4195 (2016).
40. C. Cserép, *et al.*, Microglia monitor and protect neuronal function through specialized somatic purinergic junctions. *Science (80-.).* **367**, 528–537 (2020).
41. M. W. Feinberg, *et al.*, The Kruppel-like factor KLF4 is a critical regulator of monocyte differentiation. *EMBO J.* **26**, 4138–4148 (2007).
42. T. Shichita, *et al.*, MAFB prevents excess inflammation after ischemic stroke by accelerating clearance of damage signals through MSR1. *Nat. Med.* **23**, 723–732 (2017).
43. L. I. Labzin, *et al.*, ATF3 Is a Key Regulator of Macrophage IFN Responses. *J. Immunol.* **195**, 4446–4455 (2015).
44. D. Glal, *et al.*, ATF3 Sustains IL-22-Induced STAT3 Phosphorylation to Maintain Mucosal Immunity Through Inhibiting Phosphatases. *Front. Immunol.* **9** (2018).
45. R. Heinrich, *et al.*, ATF3 Regulates the Expression of AChE During Stress. *Front. Mol. Neurosci.* **11** (2018).
46. S. Andrews, FastQC: a quality control tool for high throughput sequence data. (2010).
47. , Flexbar 3.0 – SIMD and multicore parallelization | Bioinformatics | Oxford Academic (March 13, 2020).
48. R. Patro, G. Duggal, M. I. Love, R. A. Irizarry, C. Kingsford, Salmon provides fast and bias-aware quantification of transcript expression. *Nat. Methods* **14**, 417–419 (2017).
49. W. C. Wang, *et al.*, miRExpress: analyzing high-throughput sequencing data for profiling microRNA expression. *BMC Bioinformatics* **10**, 328 (2009).
50. P. Loher, A. G. Telonis, I. Rigoutsos, MINTmap: Fast and exhaustive profiling of nuclear and mitochondrial tRNA fragments from short RNA-seq data. *Sci. Rep.* (2017) https:/doi.org/10.1038/srep41184.
51. M. L. Delignette-Muller, C. Dutang, fitdistrplus: An R package for fitting distributions. *J. Stat. Softw.* **64**, 1–34 (2015).
52. T. Bartosh, J. Ylostalo, Macrophage Inflammatory Assay. *BIO-PROTOCOL* **4** (2014).
53. M. I. Love, W. Huber, S. Anders, Moderated estimation of fold change and dispersion for RNA-seq data with DESeq2. *Genome Biol.* **15** (2014).

Figures

Figure 1. Post-stroke co-modified blood tRFs/miRs targeting cholinergic transcripts segregate into distinct clusters. A) Whole blood RNAs were collected on day 2 post-stroke from patients of the PREDICT cohort (NCT01079728)(15) and age-matched controls. B) PCA of DE tRFs/miRs in patients' blood separated stroke and control samples. C) Volcano plot of DE tRFs from stroke patients and controls (horizontal line at adjusted p = 0.05) showing upregulation of most DE tRFs. D) Volcano plot of DE miRs shows predominant downregulation in stroke patients compared with controls (horizontal line at adjusted p = 0.05). Red dots in C and D reflect Cholino-tRFs and Cholino-miRs, respectively. E) t-SNE visualization of tRF homology based on pairwise alignment scores of sequences of all detected tRNA fragments shows grouped tRFs of several specific amino acid origins.

Figure 2. RT-qPCR validation in PREDICT stroke patients of top 6 upregulated tRFs following size selection for small RNAs. A) RNA-sequencing counts normalized to the size of the library (using DESeq2(53)) of the top 6 upregulated tRFs (from left to right). Asterisks indicate adjusted p-values of Wald test via DESeq2, * $p < 0.05$, ** $p < 0.01$, *** $p < 0.001$, shown are box-plots with whiskers minimum to maximum. B) Size selection workflow for validations in a separate sub-group of PREDICT stroke patients (n=32) using the same control group (n=10); C) RT-qPCR validations using normalized expression (hsa-miR-30d-5p, hsa-let7d-5p, hsa-miR-106b-3p and hsa-miR-3615 served as house-keeping genes, see Supplementary Methods), relative to the control group (line at mean normalized expression for the control group =1) confirmed upregulation of top 6 DE tRFs identified in RNA-sequencing, ANOVA with Tukey post-hoc , * $p < 0.05$, ** $p < 0.01$, *** $p < 0.001$, box-plots with whiskers minimum to maximum.

Figure 3. Identifying blood tRFs DE post-stroke in specific cellular compartments. A)

Analysis of RNA-sequencing datasets from T lymphocytes (CD4+ T helper cells and CD8+ T cytotoxic cells), B lymphocytes (CD19+), NK cells (CD56+), monocytes (CD14+), neutrophils (CD15+) erythrocytes (CD235a+), serum, exosomes and whole blood(22) yielded a blood tRF profile. B) Definition of presence/absence of small RNAs in these blood compartments via statistical assertion of log-normal count distribution (Values between 0 and 1, closer to 1: present). C) Detailed analysis of identified tRFs found 8 sub-clusters based on cell types expressing specific molecules. D) t-SNE of all found tRFs represented by grey dots, DE tRFs identified in the PREDICT study are marked with cluster-specific color. E) t-SNE of all tRFs found, Cholino-tRFs identified in the PREDICT study are marked with cluster-specific color.

Figure 4. Monocytes express most cholinergic core and receptor genes A) Shown are web-deposited cell type-specific long RNA profiles(23), tissue-matched to reflect T lymphocytes (CD4+ T-helper cells and CD8+ T-cytotoxic cells), B lymphocytes (CD19+), NK cells (CD56+), monocytes (CD14+), and neutrophils (CD15+). B) t-SNE visualization of 15032 genes on the basis of their expression in blood-borne immune cells extrapolated from transcriptional activities in regulatory circuits(23). Genes are colored by the cell type in which their expression was highest. Cholinergic core and receptor genes were mainly found in the CD14+ monocytic compartment. C) Enrichment of post-stroke DE genes (log2FoldChange > 1.4) in circulation- and immunity-related pathways, presented as t-SNE of GO terms by their shared genes (see Supplementary Methods); color denotes t-SNE cluster, size denotes number of significant genes in term; deeper color indicates lower enrichment p-value (all p-values < 0.05). Distance between terms indicates the number of shared genes between the GO terms, closer meaning more shared genes.

Figure 5. CD14+ TF regulatory circuits reveal dichotomous miRs and tRfs influence, and murine RAW 264.7 cells show dexamethasone-suppressible tRF elevation under LPS. A)

Small RNA targeting of TFs active in CD14+ cells was analyzed using an in-house database(18). B) Force-directed network of all TFs active in CD14+ monocytes self-segregates to form largely distinct TF clusters targeted by DE tRFs and miRs in stroke patients' blood. Yellow = TF, red = TF DE in stroke patients' blood, green = miR, purple = tRF. Size of node denotes activity towards targets. C) The top 18 DE TFs in stroke patients' blood present a gradient of targeting by miRs and/or tRFs (left = 100% miR targeting, right = 100% tRF targeting; value shown as "tRF fraction – 0.5" to center on 50/50 regulation by miRs and tRFs). Size of points and color denote absolute count-change and direction of differential regulation, respectively. "C" marks TFs targeting cholinergic core or receptor genes. D) Eight DE TFs present in CD14+ monocytes are predicted not to be targeted by small RNAs. E) LPS stimulation of RAW264.7 murine macrophage cells induced clear morphology changes within 18h. Extracted RNA was subjected to size selection and cDNA synthesized from the <50 nt fraction alone. Scale bar = 100µm F) LPS-stimulated RAW264.7 cells show dexamethasone-suppressible elevated levels of post-stroke induced tRFs. Normalized RT-qPCR values (using mmu-miR-30d-5p, mmu-let7d-5p as house-keeping genes, Supplementary Methods), compared to unstimulated controls. Each dot represents 2-4 technical replicates, ANOVA with Tukey post-hoc, * $p < 0.05$, ** $p < 0.01$, *** $p < 0.001$, bar graphs +/- standard deviation (SD).

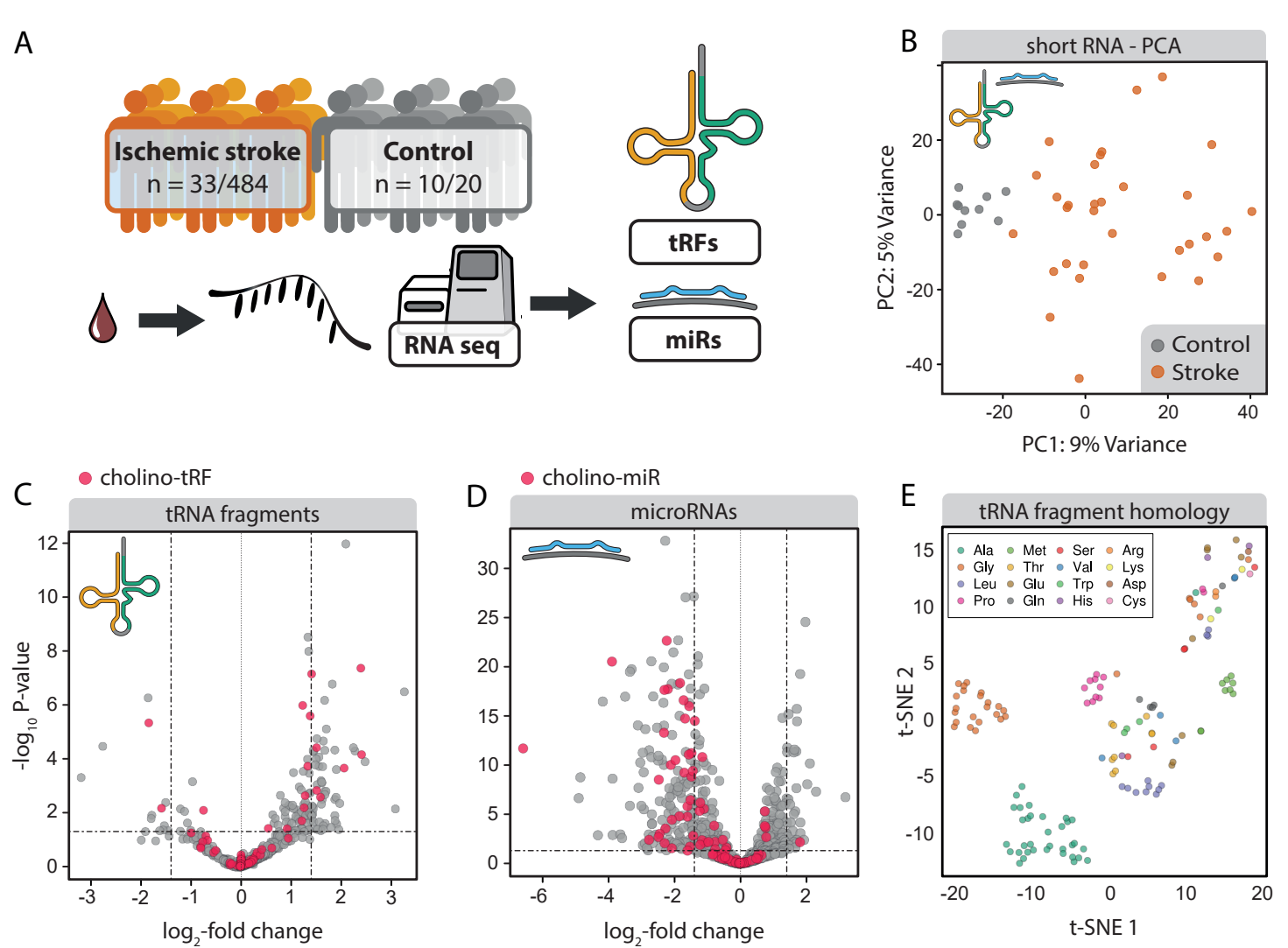
A
Ischemic stroke
n = 33/484
Control
n = 10/20
RNA seq
tRFs
miRs
B
short RNA - PCA
PC2: 5% Variance
PC1: 9% Variance
Control
Stroke
C
cholino-tRF
tRNA fragments
-log10 P-value
log2-fold change
D
cholino-miR
microRNAs
log2-fold change
E
tRNA fragment homology
Ala
Gly
Leu
Pro
Met
Thr
Glu
Gln
Ser
Val
Trp
His
Arg
Lys
Asp
Cys
t-SNE 2
t-SNE 1

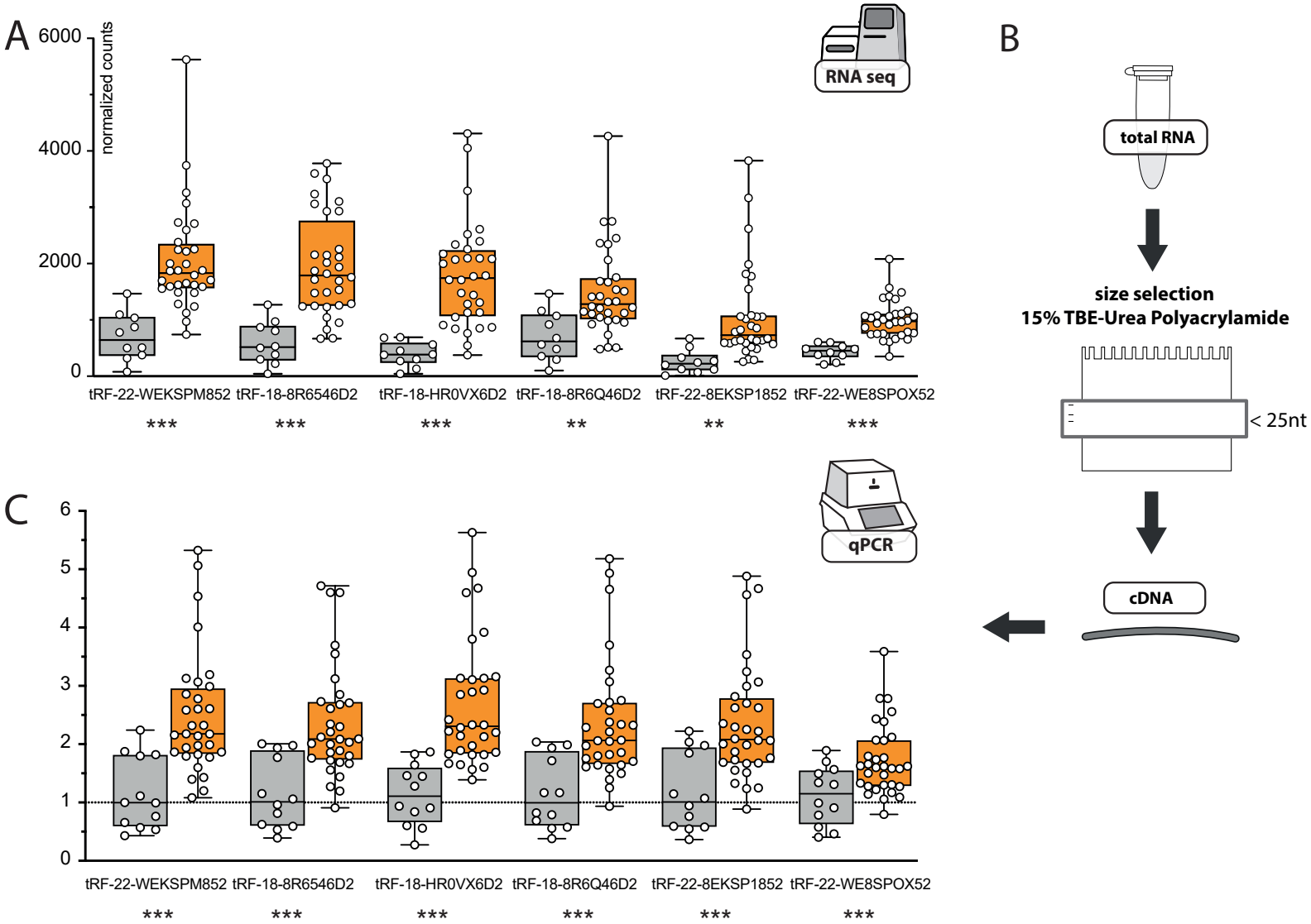
A
normalized counts
6000
4000
2000
0
RNA seq
tRF-22-WEKSPM852
tRF-18-8R6546D2
tRF-18-HR0VX6D2
tRF-18-8R6Q46D2
tRF-22-8EKSP1852
tRF-22-WE8SPOX52
***
***
***
**
**
***
B
total RNA
size selection
15% TBE-Urea Polyacrylamide
< 25nt
cDNA
C
qPCR
6
5
4
3
2
1
0
tRF-22-WEKSPM852
tRF-18-8R6546D2
tRF-18-HR0VX6D2
tRF-18-8R6Q46D2
tRF-22-8EKSP1852
tRF-22-WE8SPOX52
***
***
***
***
***
***

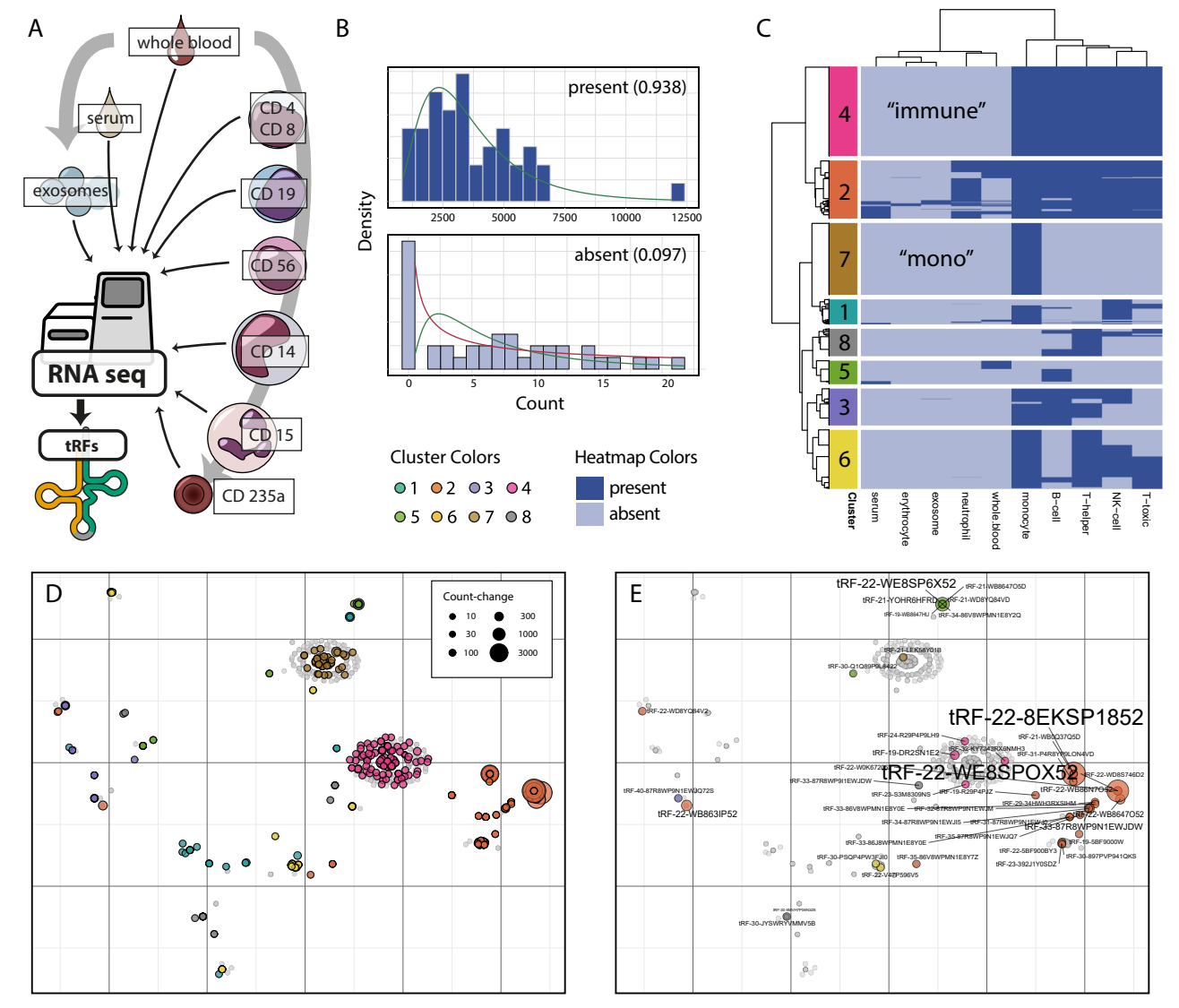
A
whole blood
serum
exosomes
CD 4
CD 8
CD 19
CD 56
CD 14
CD 15
CD 235a
RNA seq
tRFs
B
present (0.938)
absent (0.097)
Density
Count
2500
5000
7500
10000
12500
0
5
10
15
20
Cluster Colors
1 2 3 4
5 6 7 8
Heatmap Colors
present
absent
C
4
2
7
1
8
5
3
6
"immune"
"mono"
Cluster
serum
erythrocyte
exosome
neutrophil
whole blood
monocyte
B-cell
T-helper
NK-cell
T-toxic
D
Count-change
10
30
100
300
1000
3000
E
tRF-22-WE8SP6X52
tRF-21-YOHR6HFRD
tRF-21-WB8647O5D
tRF-21-WD8YQ84VD
tRF-19-WB8847HJ
tRF-34-86V8WPMN1E8Y2Q
tRF-21-LEK6W0JB
tRF-30-Q1Q89P9L84Z2
tRF-22-WD8YQ84V2
tRF-22-8EKSP1852
tRF-24-R29P4P9LH9
tRF-21-WB8Q37Q5D
tRF-19-DR25N1E2
tRF-31-K1YE43BXG9MH3
tRF-31-P4R8Y79LON4VD
tRF-22-WK6720
tRF-22-WE8SPOX52
tRF-22-WD8S746D2
tRF-33-87R8WP9I1EWJDW
tRF-40-87R8WP9N1EWQ72S
tRF-23-S3M8309NS
tRF-19-R29P4PJZ
tRF-22-WB86N7O52
tRF-22-WB863IP52
tRF-33-86V8WPMN1E8Y0E
tRF-29-34HWH3BXS9HM
tRF-22-WB8647O52
tRF-34-87R8WP9N1EWJI5
tRF-31-87R8WP9N1EWJ0
tRF-33-87R8WP9N1EWJDW
tRF-35-87R8WP9N1EWJQ7
tRF-33-86J8WPMN1E8Y0E
tRF-19-5BF9000W
tRF-22-5BF900BY3
tRF-30-PSQP4PW3FJ80
tRF-35-86V8WPMN1E8Y7Z
tRF-30-897PVP941QKS
tRF-23-392J1Y0SDZ
tRF-22-V8ZP596V5
tRF-30-JYSWRYVMMV5B

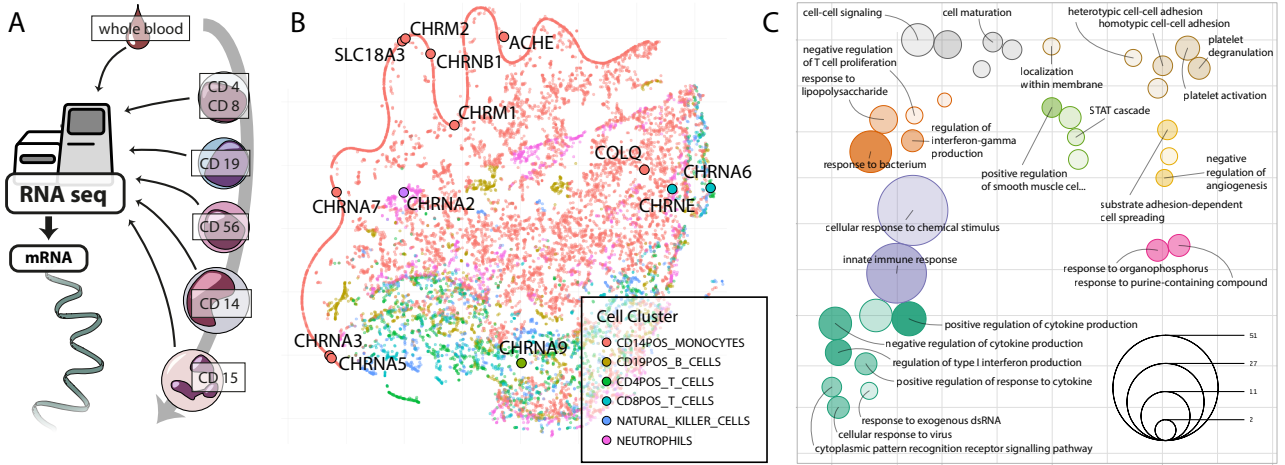
A
whole blood
CD 4
CD 8
CD 19
CD 56
CD 14
CD 15
RNA seq
mRNA
B
CHRM2
ACHE
SLC18A3
CHRNB1
CHRM1
COLQ
CHRNA6
CHRNE
CHRNA7
CHRNA2
CHRNA3
CHRNA5
CHRNA9
Cell Cluster
CD14POS_MONOCYTES
CD19POS_B_CELLS
CD4POS_T_CELLS
CD8POS_T_CELLS
NATURAL_KILLER_CELLS
NEUTROPHILS
C
cell-cell signaling
cell maturation
heterotypic cell-cell adhesion
homotypic cell-cell adhesion
platelet degranulation
negative regulation of T cell proliferation
response to lipopolysaccharide
localization within membrane
platelet activation
STAT cascade
regulation of interferon-gamma production
response to bacterium
positive regulation of smooth muscle cel...
negative regulation of angiogenesis
substrate adhesion-dependent cell spreading
cellular response to chemical stimulus
innate immune response
response to organophosphorus
response to purine-containing compound
positive regulation of cytokine production
negative regulation of cytokine production
regulation of type I interferon production
positive regulation of response to cytokine
response to exogenous dsRNA
cellular response to virus
cytoplasmic pattern recognition receptor signalling pathway
S1
Z7
L1
Z

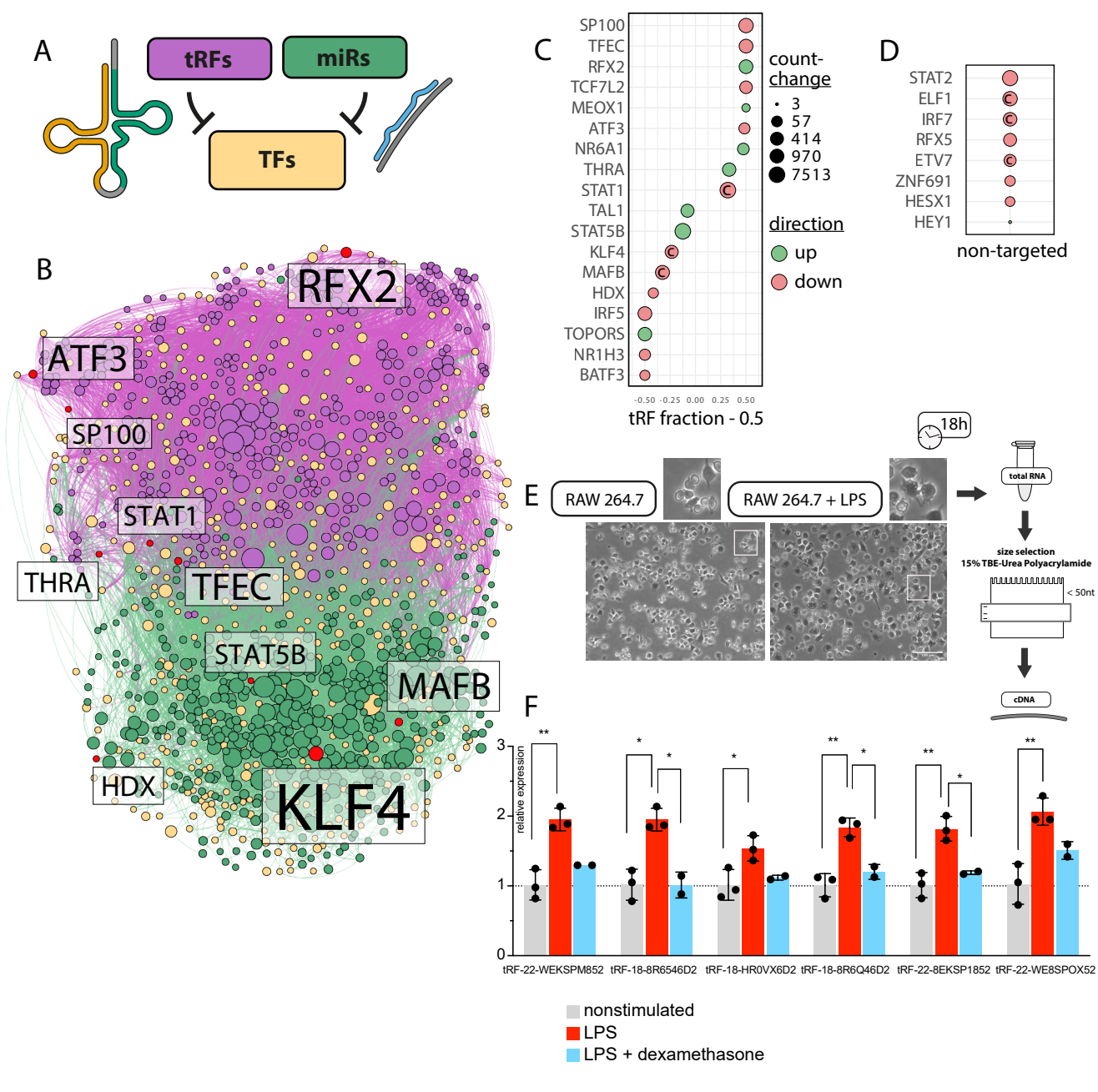
A
tRFs
miRs
TFs
B
RFX2
ATF3
SP100
STAT1
THRA
TFEC
STAT5B
MAFB
HDX
KLF4
C
SP100
TFEC
RFX2
TCF7L2
MEOX1
ATF3
NR6A1
THRA
STAT1
TAL1
STAT5B
KLF4
MAFB
HDX
IRF5
TOPORS
NR1H3
BATF3
-0.50 -0.25 0.00 0.25 0.50
tRF fraction - 0.5
count-change
3
57
414
970
7513
direction
up
down
D
STAT2
ELF1
IRF7
RFX5
ETV7
ZNF691
HESX1
HEY1
non-targeted
E
RAW 264.7
RAW 264.7 + LPS
18h
total RNA
size selection
15% TBE-Urea Polyacrylamide
< 50nt
cDNA
F
relative expression
0
1
2
3
tRF-22-WEKSPM852
tRF-18-8R6546D2
tRF-18-HR0VX6D2
tRF-18-8R6Q46D2
tRF-22-8EKSP1852
tRF-22-WE8SPOX52
nonstimulated
LPS
LPS + dexamethasone